



## ISTITUTO NAZIONALE DI RICERCA METROLOGICA Repository Istituzionale

Exploring the Role of Donor-Acceptor Interactions in Phenothiazine Organic Dyes and Their Implications for Quasi-Solid-State Dye-Sensitized Solar Cells

*Original*

Exploring the Role of Donor-Acceptor Interactions in Phenothiazine Organic Dyes and Their Implications for Quasi-Solid-State Dye-Sensitized Solar Cells / Afre, Rakesh A.; Ryu, Ka Yeon; Shin, Won Suk; Pugliese, Diego. - In: ENERGIES. - ISSN 1996-1073. - 17:24(2024). [10.3390/en17246466]

*Availability:*

This version is available at: 11696/82499 since: 2024-12-31T15:46:59Z

*Publisher:*

MDPI

*Published*

DOI:10.3390/en17246466

*Terms of use:*

This article is made available under terms and conditions as specified in the corresponding bibliographic description in the repository

*Publisher copyright*

(Article begins on next page)

## Article

# Exploring the Role of Donor–Acceptor Interactions in Phenothiazine Organic Dyes and Their Implications for Quasi-Solid-State Dye-Sensitized Solar Cells

Rakesh A. Afre <sup>1</sup> , Ka Yeon Ryu <sup>2</sup>, Won Suk Shin <sup>3</sup> and Diego Pugliese <sup>4,\*</sup> 

<sup>1</sup> Department of Engineering Science, Zeal College of Engineering and Research, Survey No. 39, Narhe-Dhayari Road, Narhe, Pune 411 041, Maharashtra, India; 79.rakesh@gmail.com

<sup>2</sup> Research Institute of Molecular Alchemy, Gyeongsang National University, 501 Jinju-daero, Gyeongsangnam-do, Jinju-Si 52828, Republic of Korea; ryuky@gnu.ac.kr

<sup>3</sup> Advanced Energy Materials Research Center, Korea Research Institute of Chemical Technology (KRICT), 141 Gajeong-ro, Yuseong-gu, Daejeon 34114, Republic of Korea; shinws@kRICT.re.kr

<sup>4</sup> National Institute of Metrological Research (INRiM), Strada delle Cacce 91, 10135 Torino, Italy

\* Correspondence: d.pugliese@inrim.it; Tel.: +39-011-3919-627

**Abstract:** This study introduces novel phenothiazine-based organic dyes, 2-LBH-100, 2-LBH-44, and 2-Ryu-4, specifically designed for quasi-solid-state dye-sensitized solar cells (QsDSSCs). Employing a donor- $\pi$ -acceptor architecture, these dyes incorporate varying electron-donating moieties, including bis(3-(hexyloxy)phenyl)amine and diphenylamino, coupled with a cyanoacrylic acid acceptor. Alkoxy substitutions in 2-LBH-100 and 2-LBH-44 enhanced solubility and dye loading on TiO<sub>2</sub>, leading to improved performance in QsDSSCs. 2-LBH-100 exhibited a power conversion efficiency (PCE) exceeding 5% with excellent stability, while 2-LBH-44 demonstrated a PCE of over 3%, increasing to 4% over time. 2-Ryu-4, with its diphenylamino donor, achieved an initial PCE of over 6%. This research highlights the crucial role of donor–acceptor interactions in optimizing organic dye design for high-performance QsDSSCs, paving the way for efficient and stable next-generation solar energy technologies.

**Keywords:** quasi-solid-state electrolytes; organic dyes; phenothiazine; donor–acceptor systems; molecular engineering; device stability



**Citation:** Afre, R.A.; Ryu, K.Y.; Shin, W.S.; Pugliese, D. Exploring the Role of Donor–Acceptor Interactions in Phenothiazine Organic Dyes and Their Implications for Quasi-Solid-State Dye-Sensitized Solar Cells. *Energies* **2024**, *17*, 6466. <https://doi.org/10.3390/en17246466>

Academic Editor: Sungjin Jo

Received: 12 November 2024

Revised: 13 December 2024

Accepted: 20 December 2024

Published: 22 December 2024



**Copyright:** © 2024 by the authors. Licensee MDPI, Basel, Switzerland. This article is an open access article distributed under the terms and conditions of the Creative Commons Attribution (CC BY) license (<https://creativecommons.org/licenses/by/4.0/>).

## 1. Introduction

Dye-sensitized solar cells (DSSCs) have garnered significant attention as a promising third-generation photovoltaic technology due to their cost-effectiveness, ease of fabrication, and environmental compatibility. Since their inception by O'Regan and Grätzel in 1991, extensive efforts have been dedicated to improving their performance, stability, and scalability for practical applications [1]. Recent research on DSSCs has shifted from basic designs to advanced configurations, including quasi-solid-state DSSCs (QsDSSCs), which address critical issues of liquid electrolyte leakage, evaporation, and instability under operational conditions. This work focuses on QsDSSCs, emphasizing their recent advances, particularly polymer blending, innovative charge transfer mechanisms, spectral engineering, and the strategic design of sensitizers, with a specific emphasis on phenothiazine-based dyes. Quasi-solid-state electrolytes have bridged the gap between liquid and solid-state DSSCs. These electrolytes combine the high ionic conductivity of liquid systems with the mechanical stability of solid systems, providing a pathway to enhance device stability without sacrificing efficiency. Recent advances in polymer blending have shown remarkable potential in fine-tuning the physicochemical properties of quasi-solid electrolytes. For example, polymers such as poly(vinylidene fluoride-co-hexafluoropropylene) (PVDF-HFP) and polyethylene oxide (PEO) have been blended with ionic liquids to optimize ionic mobility, mechanical robustness, and electrolyte/dye compatibility [2]. The incorporation of polymer-in-salt systems, where the polymer matrix acts as a scaffold for high salt content, has further enhanced the charge transfer

properties of QsDSSCs [3]. Innovative charge transfer mechanisms, such as the synergistic interplay between polymers and ionic species, have provided new avenues to improve device performance. Studies have demonstrated that the polymer matrix can facilitate better charge separation and reduce recombination losses by forming an optimal microenvironment for ion transport [4]. This mechanism also aligns with the broader trend of developing advanced electrolyte systems for sustainable and efficient QsDSSCs.

Spectral engineering has emerged as a critical area for enhancing the light-harvesting efficiency of DSSCs. Traditional dyes, though effective, often suffer from narrow absorption spectra that limit their efficiency under real-world conditions. Recent efforts have focused on designing dyes capable of capturing a broader spectrum of sunlight, particularly in the near-infrared (NIR) region, which constitutes a significant portion of solar energy [5]. Techniques such as molecular engineering, co-sensitization, and tandem DSSCs have been employed to extend the spectral response. For QsDSSCs, spectral engineering not only improves photon absorption but also ensures compatibility with the quasi-solid-state electrolyte environment. Dyes with optimized redox potentials and minimal desorption tendencies are essential for maintaining long-term device stability and efficiency. Computational studies and experimental validations have shown that spectral tuning can be achieved by introducing electron-donating and electron-withdrawing groups to the dye's molecular structure, enhancing light absorption and electron injection capabilities [6,7].

The choice of dye is pivotal for the success of QsDSSCs. Ideal sensitizers should exhibit strong absorption across the visible and NIR regions, high molar extinction coefficients, and robust anchoring groups to maintain adherence to the semiconductor surface under varying conditions. Additionally, they must possess suitable energy levels to facilitate efficient electron injection into the TiO<sub>2</sub> conduction band while regenerating through redox mediators in the quasi-solid electrolyte [8]. Phenothiazine-based dyes have shown exceptional promise in this regard. Their unique molecular framework, featuring a conjugated system and easily tunable properties, allows for significant structural modification to improve light-harvesting and charge transfer characteristics. Recent advancements in phenothiazine dyes include the introduction of auxiliary donor or acceptor groups to enhance intramolecular charge transfer and broaden absorption spectra [9]. For instance, dyes incorporating bulky alkyl groups have demonstrated improved photostability and reduced recombination by minimizing aggregation effects on the semiconductor surface [10]. Phenothiazine dyes have garnered attention due to their versatility in molecular design and compatibility with quasi-solid-state systems. Recent studies have explored their application in QsDSSCs, leveraging their ability to interact effectively with polymer electrolytes. For example, the introduction of triphenylamine or carbazole moieties into phenothiazine frameworks has improved dye performance by facilitating better light absorption and charge transport. Additionally, efforts to functionalize phenothiazine dyes with electron-rich groups have resulted in dyes with enhanced redox stability and dye regeneration efficiency [11–13].

Another notable advancement in phenothiazine dyes is their ability to mitigate the impact of charge recombination. Molecular engineering strategies, such as incorporating bulky substituents or steric hindrances, have proven effective in reducing charge recombination at the TiO<sub>2</sub> interface, thereby enhancing the open-circuit voltage ( $V_{oc}$ ) and overall device efficiency [14]. Despite significant progress, QsDSSCs face several challenges that necessitate further investigation. Achieving long-term stability under operational conditions remains a primary concern. While quasi-solid-state electrolytes mitigate leakage issues, their ionic conductivity and mechanical robustness must be optimized to ensure consistent performance over extended periods. Additionally, the development of dyes with enhanced stability, compatibility with quasi-solid electrolytes, and minimal degradation tendencies is critical for advancing QsDSSCs toward commercialization. Future research should focus on integrating novel materials, such as hybrid organic–inorganic electrolytes and advanced nanostructured semiconductors, to improve the performance and scalability of QsDSSCs. Furthermore, a deeper understanding of interfacial charge dynamics and recombination mechanisms is essential to guide the design of next-generation dyes and electrolytes.

This study investigates three novel phenothiazine dyes, namely 2-LBH-100, 2-LBH-44, and 2-Ryu-4, featuring a common phenothiazine core and cyanoacrylic acid acceptor but differing in their donor moieties. The dyes were synthesized, characterized, and incorporated into QsDSSCs to evaluate their photovoltaic performance. The impact of donor structure on light absorption, quantum efficiency, and device performance and stability was systematically investigated. The findings of this study provide valuable insights into the design and development of efficient and stable organic dyes for next-generation photovoltaic applications.

## 2. Materials and Methods

The Materials and Methods section is the same as in our recently published work [15], with the only change in different organic dyes having hexyloxy, benzyloxy, and diphenylamino as electron-donating moieties to understand their effect on QsDSSCs' performance and stability over time. However, for the sake of major completeness and of making the information more easily accessible, it has been decided to report the main details regarding the assembly, characterization, and stability study of the DSSCs in the subsections below. It is also worth mentioning that the optical absorbance of the TiO<sub>2</sub> photoelectrodes sensitized with the three different dyes was obtained by the ultraviolet–visible (UV–Vis) spectrophotometer UV-1800, Shimadzu Scientific Instruments, Kyoto, Japan.

### 2.1. Assembly and Characterization of DSSCs

The assembly of DSSCs involved placing an electrolyte layer between a dye-sensitized TiO<sub>2</sub> photoelectrode and a Pt counter electrode. To ensure adequate filling of the electrolyte, a surlyn film (Solaronix, Aubonne, Switzerland) was utilized to create a gap between the two electrodes. Various electrolytes were tested to assess their impact on device performance, including 1,2-dimethyl-3-propylimidazolium iodide (DMPII) liquid electrolyte and PVDF-HFP gel polymer electrolytes with different molecular weight: 86,000 g/mol (PVH70), 90,000 g/mol (PVH80), and 455,000 g/mol (PVDF-HFP).

The devices' current density–voltage ( $J$ – $V$ ) curves were obtained utilizing a Keithley 2400 source measure unit (SMU) (Tektronix, Seoul, Republic of Korea) in conjunction with a solar simulator (K201 LAB55, McScience Inc., Yeongtong, Republic of Korea). An irradiation level of 100 mW/cm<sup>2</sup>, guaranteed by a 150 W xenon (Xe) short-arc lamp filtered by an air mass 1.5 G filter (McScience Inc., Yeongtong, Republic of Korea), was used, which satisfies the Class AAA American Society for Testing and Materials Standards. The calibration of light intensity was performed with a Si reference cell (K801S-K302, McScience Inc., Yeongtong, Republic of Korea). To measure the incident photon-to-electron conversion efficiency (IPCE) curves, a spectral measurement system (K3100 IQX, McScience Inc., Yeongtong, Republic of Korea) was employed, which utilized monochromatic light from a 300 W Xe arc lamp, filtered through an optical chopper (MC2000, Thorlabs, Newton, NJ, USA) and a monochromator (CS130B-1-FH, Newport, Daejeon, Republic of Korea).

### 2.2. Stability Study of DSSCs

The stability analysis of the liquid and quasi-solid-state DSSCs was performed by storing the cells at 70 °C in oven with a humidity of 40–45%, and data were gathered at 24 h intervals.

## 3. Results

### 3.1. Chemical Structures of the Dyes

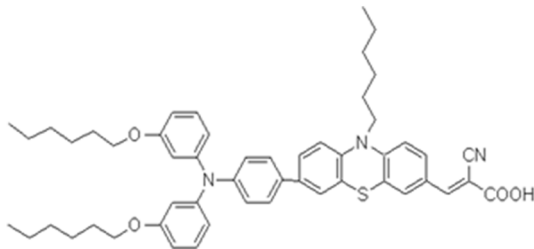
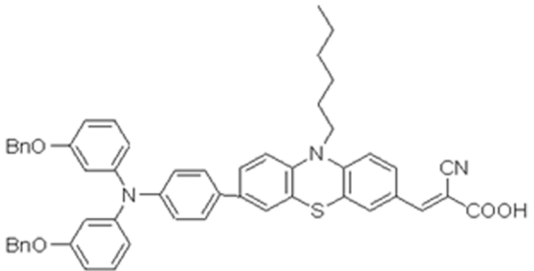
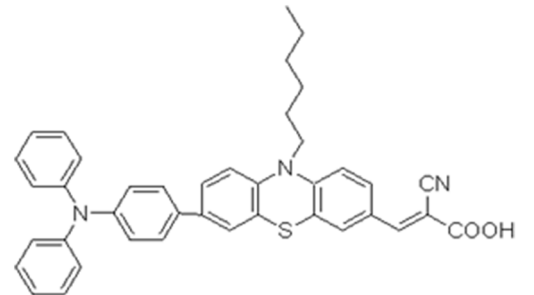
DSSCs have emerged as a promising alternative to conventional silicon-based solar cells due to their potential for low-cost fabrication and high-power conversion efficiency. In particular, QsDSSCs offer advantages such as improved stability and reduced leakage compared to their liquid electrolyte counterparts. However, achieving high efficiencies in QsDSSCs remains a challenge, necessitating the development of novel dye materials with tailored optoelectronic properties. Organic dyes based on the phenothiazine scaffold have

garnered significant attention as sensitizers for DSSCs due to their strong electron-donating ability, tunable energy levels, and high molar extinction coefficients. The performance of these dyes is strongly influenced by the interplay between the electron-donating and electron-accepting moieties within the molecule.

This research investigates three novel phenothiazine dyes, 2-LBH-100, 2-LBH-44, and 2-Ryu-4, to elucidate the impact of donor–acceptor interactions on their photovoltaic performance in QsDSSCs. All the three dyes share a common structural motif consisting of a phenothiazine core as the electron donor, a cyanoacrylic acid group as the electron acceptor, and a phenyl ring as the  $\pi$ -bridge linking the two. However, they differ in the substituents attached to the donor moiety, allowing us to systematically investigate the influence of donor strength on the dyes' properties and device performance. 2-LBH-100 features two 3-(hexyloxy)phenyl groups attached to the nitrogen atom of the phenothiazine core. These bulky, electron-rich substituents serve two primary purposes. First, they enhance the electron-donating ability of the phenothiazine core, leading to a red-shifted absorption spectrum and improved light-harvesting capabilities. Second, the bulky hexyl chains can hinder dye aggregation on the TiO<sub>2</sub> surface, which is known to reduce device efficiency by increasing charge recombination losses [16,17].

The structures of phenothiazine dyes and their chemical name are reported in Table 1 together with their molecular weight (M.W.).

**Table 1.** Chemical structures and names of organic phenothiazine dyes having different electron donating moieties.

Chemical Structure	Chemical Name
	(E)-3-(7-(4-(bis(3-(hexyloxy)phenyl)amino)phenyl)-10-hexyl-10H-phenothiazin-3-yl)-2-cyanoacrylic acid (2-LBH-100) M.W.: 822.11 g/mol
	(E)-3-(7-(4-(bis(benzyloxy)phenyl)amino)phenyl)-10-hexyl-10H-phenothiazin-3-yl)-2-cyanoacrylic acid (2-LBH-44) M.W.: 834.03 g/mol
	(E)-2-cyano-3-(7-(4-(diphenylamino)phenyl)-10-hexyl-10H-phenothiazin-3-yl)acrylic acid (2-Ryu-4) M.W.: 621.79 g/mol

2-LBH-44 is structurally similar to 2-LBH-100 but with benzyloxy groups instead of hexyloxy groups. The shorter and less electron-donating benzyloxy groups are expected to result in a blue-shifted absorption spectrum and slightly lower electron-donating ability compared to 2-LBH-100. However, the benzyloxy groups still provide steric hin-

drance to minimize dye aggregation. 2-Ryu-4 represents a significant departure from the other two dyes, featuring two simple phenyl groups attached to the phenothiazine nitrogen. This dye serves as a reference point, allowing us to directly assess the impact of the alkoxy substituents in 2-LBH-100 and 2-LBH-44. The absence of electron-donating alkoxy groups is expected to result in a further blue-shifted absorption spectrum and the weakest electron-donating ability among the three dyes. By systematically comparing the photovoltaic performance of QsDSSCs fabricated with these three dyes, a comprehensive structure–property relationship is aimed to be established.

### 3.2. *J–V Characteristics of DSSCs with Phenothiazine Dyes and DMPII-Based Liquid and Quasi-Solid-State Electrolytes*

Table 2 summarizes the main photovoltaic parameters for DSSCs employing phenothiazine-based dyes, specifically, 2-LBH-100, 2-LBH-44, and 2-Ryu-4, as well as DMPII liquid electrolyte in conjunction with various-molecular-weight PVDF-HFP polymers: 86,000 g/mol (PVH70), 90,000 g/mol (PVH80), and 455,000 g/mol (PVDF-HFP).

**Table 2.** Main photovoltaic parameters of DSSCs using organic phenothiazine dyes as the sensitizer and DMPII with and without different-molecular-weight PVDF-HFP polymers as the electrolyte.

Sample No.	Dye	Electrolyte	Day 1				Day 2				Day 3			
			$V_{oc}$ [V]	$J_{sc}$ [mA/cm <sup>2</sup> ]	FF	PCE [%]	$V_{oc}$ [V]	$J_{sc}$ [mA/cm <sup>2</sup> ]	FF	PCE [%]	$V_{oc}$ [V]	$J_{sc}$ [mA/cm <sup>2</sup> ]	FF	PCE [%]
R1	2-LBH-100	D-liq.	0.74	10.10	0.64	<b>4.81</b>	0.76	10.19	0.66	<b>5.15</b>	0.77	10.28	0.67	<b>5.26</b>
R2		PVH70	0.73	10.13	0.64	<b>4.74</b>	0.75	10.20	0.65	<b>4.99</b>	0.76	10.17	0.66	<b>5.07</b>
R3		PVH80	0.74	9.70	0.63	<b>4.56</b>	0.77	10.28	0.65	<b>5.16</b>	0.78	10.25	0.65	<b>5.21</b>
R4		PVDF-HFP	0.66	10.77	0.59	<b>4.15</b>	0.66	10.57	0.61	<b>4.29</b>	0.66	10.27	0.60	<b>4.09</b>
R5	2-LBH-44	D-liq.	0.67	7.28	0.62	<b>3.05</b>	0.68	7.74	0.64	<b>3.37</b>	0.69	8.09	0.64	<b>3.55</b>
R6		PVH70	0.65	7.61	0.61	<b>3.01</b>	0.66	8.19	0.62	<b>3.34</b>	0.66	8.55	0.62	<b>3.54</b>
R7		PVH80	0.66	6.90	0.63	<b>2.84</b>	0.67	7.39	0.63	<b>3.11</b>	0.67	7.56	0.63	<b>3.22</b>
R8		PVDF-HFP	0.61	8.82	0.57	<b>3.06</b>	0.61	9.23	0.58	<b>3.26</b>	0.62	9.07	0.58	<b>3.25</b>
R9	2-Ryu-4	D-liq.	0.81	11.98	0.63	<b>6.12</b>	0.81	12.01	0.64	<b>6.24</b>	0.81	12.06	0.65	<b>6.38</b>
R10		PVH70	0.79	12.12	0.63	<b>6.08</b>	0.80	12.11	0.65	<b>6.29</b>	0.80	12.04	0.65	<b>6.28</b>
R11		PVH80	0.79	12.20	0.62	<b>5.98</b>	0.80	12.13	0.63	<b>6.15</b>	0.80	12.05	0.62	<b>6.06</b>
R12		PVDF-HFP	0.69	13.06	0.58	<b>5.32</b>	0.70	12.91	0.60	<b>5.43</b>	0.70	12.66	0.61	<b>5.42</b>

The *J–V* curves illustrated in Figure 1 highlight the significant influence of dye selection and electrolyte composition on the efficiency and stability of DSSCs. Among the tested dyes, 2-Ryu-4 exhibited the highest performance across all measured parameters, including  $V_{oc}$ , short-circuit current density ( $J_{sc}$ ), and overall power conversion efficiency (PCE). This can be attributed to its robust donor moiety, which enhanced the charge transfer capabilities. In contrast, 2-LBH-44 demonstrated lower performance metrics, indicating that the nature of the donor substituent is crucial for optimizing device efficiency.

The choice of electrolyte also played a pivotal role in refining device performance. The PVH70 and PVH80 electrolytes showed potential for improving stability and efficiency over time compared to the liquid electrolyte baseline. For instance, 2-LBH-100 maintained consistent  $V_{oc}$  values from 0.73 to 0.78 V over three days, with the highest  $V_{oc}$  of 0.78 V observed on day three with PVH80. This stability suggests effective dye–electrolyte interactions that enhanced charge transfer efficiency.  $J_{sc}$  values for 2-LBH-100 remained relatively stable, increasing slightly from 10.10 to 10.28 mA/cm<sup>2</sup>, while fill factor (FF) fluctuated between 0.63 and 0.67. The maximum PCE achieved with this dye was 5.26% using the liquid electrolyte on day three, confirming its capability for stable output under operational conditions. Conversely, 2-LBH-44 exhibited  $V_{oc}$  values ranging from 0.65 to 0.69 V, with a peak  $J_{sc}$  of only 8.55 mA/cm<sup>2</sup> when paired with PVH70 on day three. The FF remained consistent at around 0.61 to 0.64, resulting in a maximum PCE of 3.55% with the liquid electrolyte. The lower efficiency of this dye was likely due to its weaker electron-donating ability, which limited electron injection efficiency. In contrast, 2-Ryu-4 consistently achieved higher  $V_{oc}$  values of

up to 0.81 V across all days when using the liquid electrolyte. It also reached a peak  $J_{sc}$  of 13.06 mA/cm<sup>2</sup> with PVDF-HFP on day one and an overall PCE of 6.38% by day three. This superior performance underscores its effective electron transfer facilitated by a strong donor moiety. The data indicate that while PVH80 generally enhanced  $V_{oc}$  and  $J_{sc}$  across all dyes, particularly for 2-LBH-100 and 2-Ryu-4, the PVDF-HFP electrolyte improved  $J_{sc}$  but reduced FF due to higher series resistance or suboptimal ionic conductivity.

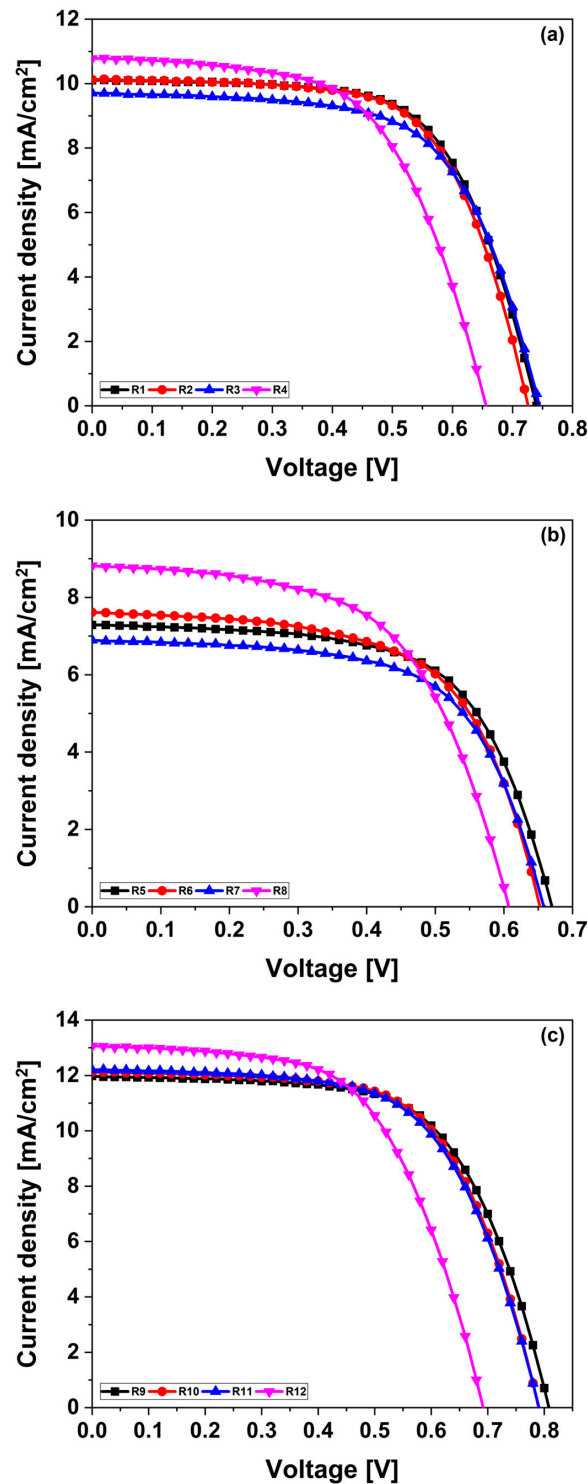


**Figure 1.**  $J$ - $V$  characteristics of DSSCs using liquid DMPII electrolytes with and without PVDF-HFP with different molecular weights and (a) 2-LBH-100, (b) 2-LBH-44, and (c) 2-Ryu-4 organic phenothiazine dyes as the sensitizer.

Overall, these findings illustrate that the molecular structure of phenothiazine dyes significantly influenced photovoltaic performance; dyes with stronger electron-donating substituents yielded superior efficiencies compared to those with weaker donors like in the case of 2-LBH-44 [16,18]. Furthermore, the choice of the electrolyte critically affected device performance, with quasi-solid-state electrolytes such as PVH70 and PVH80 providing improvements in stability and efficiency throughout the testing period. These insights align with previous studies emphasizing the importance of dye–electrolyte interactions in optimizing QsDSSCs' performance. The stable PCE values observed across three days suggest that these devices could deliver reliable performance in practical applications; however, further optimization of electrolyte compositions may be necessary to fully harness their potential. The results highlight that selecting dyes with strong electron-donating abilities and optimizing electrolyte composition are key strategies for enhancing charge transport and minimizing recombination losses.

### 3.3. DSSCs with 2-LBH-100 Phenothiazine Dye and with and Without PVDF-HFP with Different Molecular Weights in DMPII Electrolyte

#### 3.3.1. UV–Vis Absorption and IPCE Spectra

UV–Vis absorption and IPCE spectra are critical for understanding the light-harvesting capabilities and charge generation efficiency in DSSCs. The UV–Vis absorption spectrum of (E)-3-(7-(4-(bis(3-(hexyloxy)phenyl)amino) phenyl)-10-hexyl-10H-phenothiazin-3-yl)-2-cyanoacrylic acid (2-LBH-100) dye deposited on TiO<sub>2</sub> film and the IPCE spectra for DSSCs without and with different molecular weights of the PVDF-HFP polymer incorporated in the electrolyte are reported in Figure 2. The electrolyte composition includes 0.1 M iodine, 0.5 M N-methylbenzimidazole, and 0.6 M ionic liquid-DMPII, and it was designed to facilitate efficient charge transport while minimizing recombination losses.

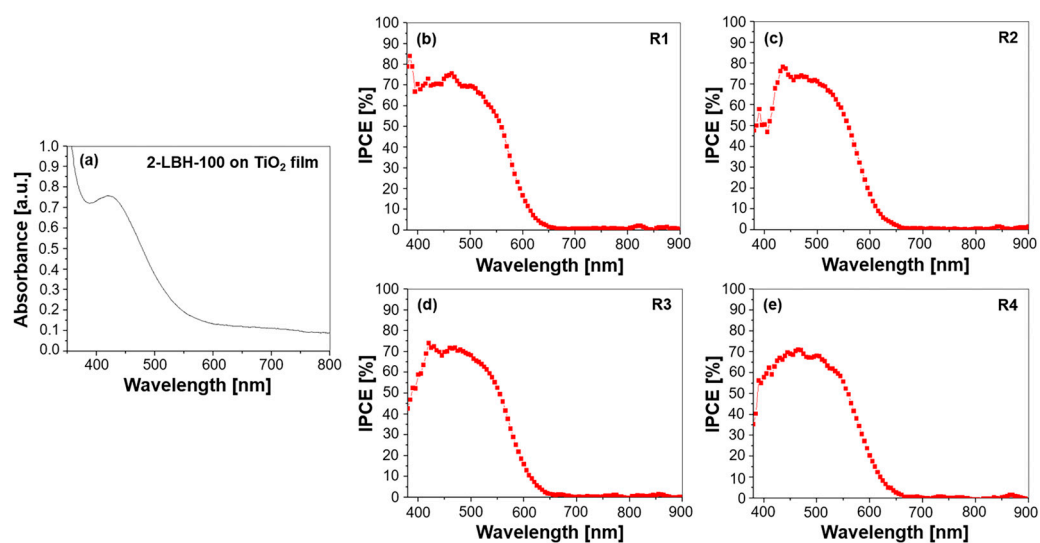


**Figure 2.** (a) UV–Vis absorption spectrum of the 2-LBH-100 phenothiazine dye adsorbed on a TiO<sub>2</sub> film and IPCE spectra for DSSCs employing 2-LBH-100 with various electrolytes: (b) R1—DMPII, (c) R2—DMPII + PVH70, (d) R3—DMPII + PVH80, and (e) R4—DMPII + PVDF-HFP.

The UV-Vis absorption spectrum depicted in Figure 2a characterizes the light-harvesting capability of the 2-LBH-100 dye adsorbed on the TiO<sub>2</sub> film. More in detail, it reveals the wavelengths of light absorbed by the dye, with the peak absorbance indicating the most efficiently absorbed wavelengths. The absorption onset, where absorption begins to increase significantly, provides an estimate of the dye's band gap. A prominent absorption band between 400 and 600 nm, peaking at approximately 450–500 nm, was observed. This absorption is characteristic of  $\pi$ - $\pi^*$  transitions within the phenothiazine chromophore, enabling the efficient harvesting of visible light. The absorption tail extending beyond 600 nm



suggests potential for capturing longer wavelengths, further enhancing light absorption. The electron-donating hexyl chains on the phenothiazine core contributed to this red-shifted absorption and improved dye solubility, facilitating interaction with the TiO<sub>2</sub> surface [19]. The incorporation of PVDF-HFP-based gel electrolytes with varying molecular weights (PVH70, PVH80, PVDF-HFP) was expected to lead to minor changes in the absorption profile. Specifically, a slight decrease in absorption intensity with PVH70 and PVH80, possibly due to interactions with the polymer matrix, should occur. However, the strong absorption within the 400–600 nm range was maintained across all electrolyte compositions, as evidenced by the IPCE spectra in Figure 2b–e, confirming efficient photon capture. This consistent absorption behavior indicates that the dye's light-harvesting capabilities are largely preserved despite the variations in the electrolyte composition [20,21].

The IPCE spectra (Figure 2b–e) provide a direct measure of the device's ability to convert absorbed photons into an electrical current. The IPCE is wavelength-dependent and represents the ratio of generated electrons to incident photons at each wavelength. The IPCE onset, typically at a longer wavelength than the absorption onset, reflects the minimum photon energy required to generate a current in the device. This difference arises because the IPCE considers factors beyond light absorption, such as charge injection and collection efficiencies. The reference cell (R1) with the DMPII liquid electrolyte exhibited a high IPCE, peaking around 80% at approximately 480 nm, correlating well with the dye's absorption peak. This high IPCE confirms efficient photon-to-current conversion. Incorporating PVDF-HFP-based gel electrolytes with increasing molecular weights (R2–R4) led to a progressive decrease in peak IPCE (77, 74, and 72% for PVH70, PVH80, and PVDF-HFP, respectively). This trend suggests that the increasing polymer concentration and molecular weight hindered ion transport within the electrolyte, affecting charge collection efficiency [22]. While the IPCE onset remained relatively consistent across all devices, the decreasing peak IPCE values indicate that fewer incident photons were being converted into current, likely due to increased recombination losses or reduced ion mobility in the more viscous gel electrolytes. Despite this reduction, the 2-LBH-100 dye maintained reasonable light-to-current conversion even with the highest-molecular-weight polymer, demonstrating its potential for use in QsDSSCs. The decrease in IPCE beyond 600 nm for all devices corresponds to the declining absorption of the dye in the NIR region.

### 3.3.2. Stability Study

The stability study of the 2-LBH-100 DSSCs with the liquid DMPII electrolyte and with gel polymer electrolytes with different molecular weights (86,000, 90,000, and 455,000 g/mol) is shown in Figure 3.

The stability study demonstrated a complex interaction between the electrolyte's molecular structure and the photovoltaic performance over time. The primary photovoltaic parameters under investigation were the  $V_{oc}$ ,  $J_{sc}$ , FF, and overall PCE, measured after 650 h of continuous operation under ambient conditions. Cells R1 (liquid electrolyte), R2, R3, and R4 (with varying polymer molecular weights) present an insightful comparison of how electrolyte composition influenced device stability and efficiency over time.

$V_{oc}$ , a critical factor in determining the energy output of a solar cell, is influenced by the electronic interactions at the TiO<sub>2</sub>/electrolyte interface. Over 650 h, the liquid electrolyte-based cell (R1) showed a 3% increase in  $V_{oc}$ , which can be attributed to the optimized electron injection and reduced recombination rates facilitated by the DMPII electrolyte. However, the quasi-solid-state cells with PVDF-HFP polymers exhibited more significant improvements in  $V_{oc}$ . The R2 cell, with a polymer molecular weight of 86,000 g/mol, showed a 6% increase in  $V_{oc}$ . This improvement can be attributed to the formation of a stable electrolyte interface that reduced charge recombination. The slightly higher-molecular-weight polymer in R3 (90,000 g/mol) resulted in a 3% increase in  $V_{oc}$ , likely due to an optimal balance between ion transport and recombination suppression. Interestingly, the highest-molecular-weight polymer in R4 (455,000 g/mol) resulted in no change in  $V_{oc}$ .

suggesting that while the polymer's dense network may have improved structural stability, it hindered efficient ion diffusion, which limited further enhancement in  $V_{oc}$ .

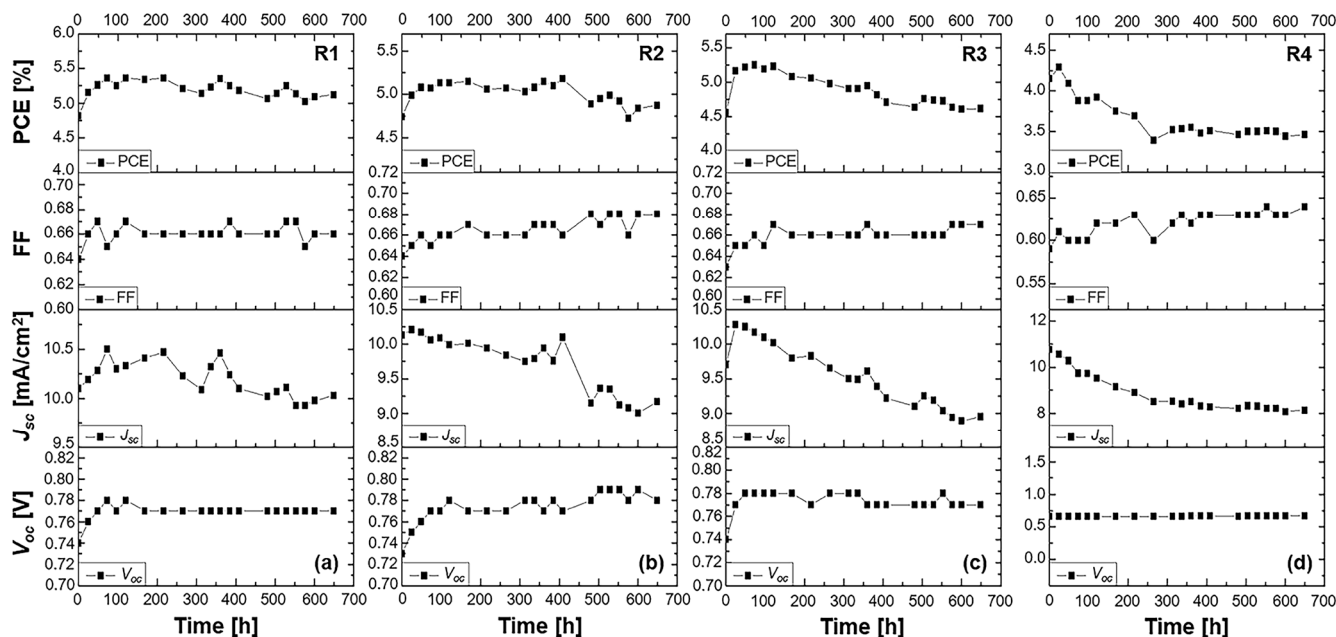


**Figure 3.** Stability study of 2-LBH-100 DSSCs measured under ambient conditions for over 600 h. Performance of (a) a liquid DMPII electrolyte-based DSSC (R1) and of QsDSSCs employing PVDF-HFP-based gel electrolytes with varying molecular weights: (b) R2—DMPII + PVH70, (c) R3—DMPII + PVH80, and (d) R4—DMPII + PVDF-HFP.

The FF, which reflects the cell's ability to extract and utilize photogenerated charge carriers, showed more significant improvement across all cells. In R1, the FF increased by 3%, indicating that the liquid electrolyte provided a moderately efficient charge extraction environment. R2 and R3, with polymer molecular weights of 86,000 and 90,000 g/mol, showed FF increases of 4 and 4.5%, respectively. This trend indicates that the semi-crystalline structure of the polymer enhanced charge carrier mobility by forming efficient ion-conductive pathways, thus reducing internal resistance. In R4, the FF saw a more significant increase of 6%, likely due to the high viscosity of the polymer, which stabilized the device and minimized leakage currents. However, this came at the cost of compromised ion transport efficiency, which impacted other parameters such as  $J_{sc}$ .

The  $J_{sc}$  trends across the different cells highlight the challenges of maintaining high charge generation efficiency over time. In the liquid electrolyte-based cell R1,  $J_{sc}$  initially increased by 5% before stabilizing. This behavior is indicative of the liquid electrolyte's capacity for continuous ionic conduction, allowing for efficient dye regeneration and charge collection [23]. However, in the quasi-solid-state cells, the introduction of the PVDF-HFP polymer significantly impacted the  $J_{sc}$ . In R2, with a polymer molecular weight of 86,000 g/mol,  $J_{sc}$  decreased by 14% after more than 600 h. This reduction suggests that the polymer's semi-crystalline structure, while stabilizing the electrolyte, may have hindered ionic movement and reduced the efficiency of dye regeneration over time, resulting in a lower photocurrent. A similar trend was observed in R3, where  $J_{sc}$  decreased by 7.5%, likely due to similar issues with ionic conductivity in the polymer matrix. In R4, with the highest-molecular-weight polymer,  $J_{sc}$  saw the most significant drop of 28%. The higher viscosity of the polymer at this molecular weight severely restricted ion transport, resulting in poor dye regeneration and reduced charge collection efficiency, leading to a dramatic reduction in  $J_{sc}$ .

Despite the decreases in  $J_{sc}$ , the PCE across all cells showed varying degrees of initial improvement. In R1, the PCE increased by 7%, reflecting the relatively stable performance of the liquid electrolyte in maintaining efficient charge transport over time. Among the

polymer-based cells, R2 saw a 3% increase in PCE, indicating that the  $V_{oc}$  and FF improvements partially compensated for the reduction in  $J_{sc}$ . The PCE increase in R3 was more modest, at 2.5%, suggesting that while the polymer matrix provided stability, the loss in  $J_{sc}$  was too significant to be fully offset by gains in  $V_{oc}$  and FF. In R4, the PCE decreased by 17%, reflecting the severe limitations imposed by the high-molecular-weight polymer on ion diffusion and charge generation, which could not be compensated for by the slight improvement in FF. Finally, the stability study of QsDSSCs using the 2-LBH-100 dye and PVDF-HFP polymer electrolytes revealed that while quasi-solid-state electrolytes offered improved stability and enhanced  $V_{oc}$  and FF, the choice of polymer molecular weight played a crucial role in determining overall device performance. Low- to medium-molecular-weight polymers (86,000 to 90,000 g/mol) provided a reasonable balance between stability and performance, resulting in moderate improvements in PCE. However, excessively high-molecular-weight polymers (455,000 g/mol) led to significant reductions in  $J_{sc}$  and, consequently, in PCE, due to the severe restrictions they placed on ionic mobility. These findings suggest that further optimization of polymer electrolytes is necessary to achieve an optimal balance between stability and performance in QsDSSCs.

### 3.4. DSSCs with 2-LBH-44 Phenothiazine Dye and with and Without PVDF-HFP with Different Molecular Weights in DMPII Electrolyte

#### 3.4.1. UV-Vis Absorption and IPCE Spectra

The UV-Vis absorption spectrum of the (E)-3-(7-(4-(bis(3-(benzyloxy)phenyl)amino)phenyl)-10-hexyl-10H-phenothiazin-3-yl)-2-cyanoacrylic acid (2-LBH-44) dye deposited on  $TiO_2$  film and the IPCE spectra for DSSCs in the absence and in the presence of the PVDF-HFP polymer with different molecular weights incorporated in the liquid electrolyte are depicted in Figure 4.

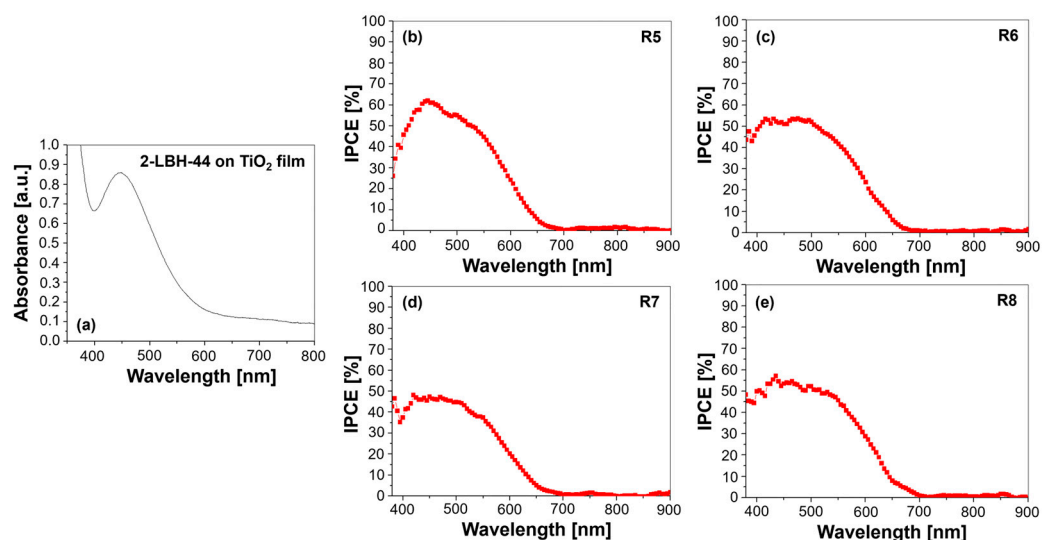


**Figure 4.** (a) UV-Vis absorption spectrum of the 2-LBH-44 phenothiazine dye adsorbed on a  $TiO_2$  film and IPCE spectra for DSSCs employing 2-LBH-44 with various electrolytes: (b) R5—DMPII, (c) R6—DMPII + PVH70, (d) R7—DMPII + PVH80, and (e) R8—DMPII + PVDF-HFP.

The UV-Vis absorption spectrum (Figure 4a) of the 2-LBH-44 dye provides information about its light-harvesting properties. The onset of the absorption spectrum, i.e., the wavelength at which absorption begins to increase significantly, provides an estimate of the dye's band gap. The broad absorption profile from 400 to 700 nm, attributed to the dye's conjugated structure, demonstrated its ability to harvest light across a wide range of visible spectrum. The benzyloxy groups likely contributed to the observed red-shift, extending the absorption range and potentially improving light harvesting [24]. The influence of the PVDF-HFP polymer molecular weight on the absorption spectrum should be described more precisely. While

lower-molecular-weight polymers might improve dye dispersion and reduce aggregation, leading to enhanced absorption, higher-molecular-weight polymers could increase viscosity and hinder ionic mobility, potentially decreasing absorption due to aggregation.

The IPCE spectra (Figure 4b–e) provide a direct measure of the device’s ability to convert absorbed photons into electrical current. The IPCE is wavelength-dependent and represents the ratio of generated electrons to incident photons at each wavelength. The wavelength at which photocurrent starts to be generated, known as IPCE onset, is usually longer than the absorption onset. This discrepancy results from the IPCE taking into account factors like charge injection and collection efficiencies that go beyond light absorption. The R5 cell with the DMPII liquid electrolyte exhibited a peak IPCE that correlates well with the UV–Vis absorption spectrum, indicating efficient charge separation and transport. The introduction of PVDF-HFP in R6 led to variations in IPCE performance, with enhanced values across a broader spectral range compared to R5. This suggests that the lower-molecular-weight PVDF-HFP facilitated better ionic conductivity and charge transport. However, increasing the molecular weight in R7 and R8 might introduce trade-offs. While the increased viscosity could hinder ion mobility, affecting overall performance, other factors, such as improved dye dispersion or reduced recombination, could also influence the IPCE. These findings highlight how molecular design and polymer interactions can significantly impact the efficiency and stability of DSSCs [11]. The interplay between UV absorption characteristics and quantum efficiency metrics revealed critical insights into how variations in electrolyte composition affected the performance of QsDSSCs using 2-LBH-44. Optimizing these parameters is essential for advancing solar cell technology and improving energy conversion efficiencies in practical applications. The molecular weight of PVDF-HFP significantly affected the stability of the 2-LBH-44 dye in DSSCs due to its influence on the electrolyte’s viscosity, ionic conductivity, and polymer–dye interactions.

### 3.4.2. Stability Study

The stability study of DSSCs utilizing the phenothiazine-based dye 2-LBH-44 in combination with the liquid DMPII electrolyte without and with varying molecular weights of PVDF-HFP, reported in Figure 5, reveals fascinating insights into the long-term performance of these devices.

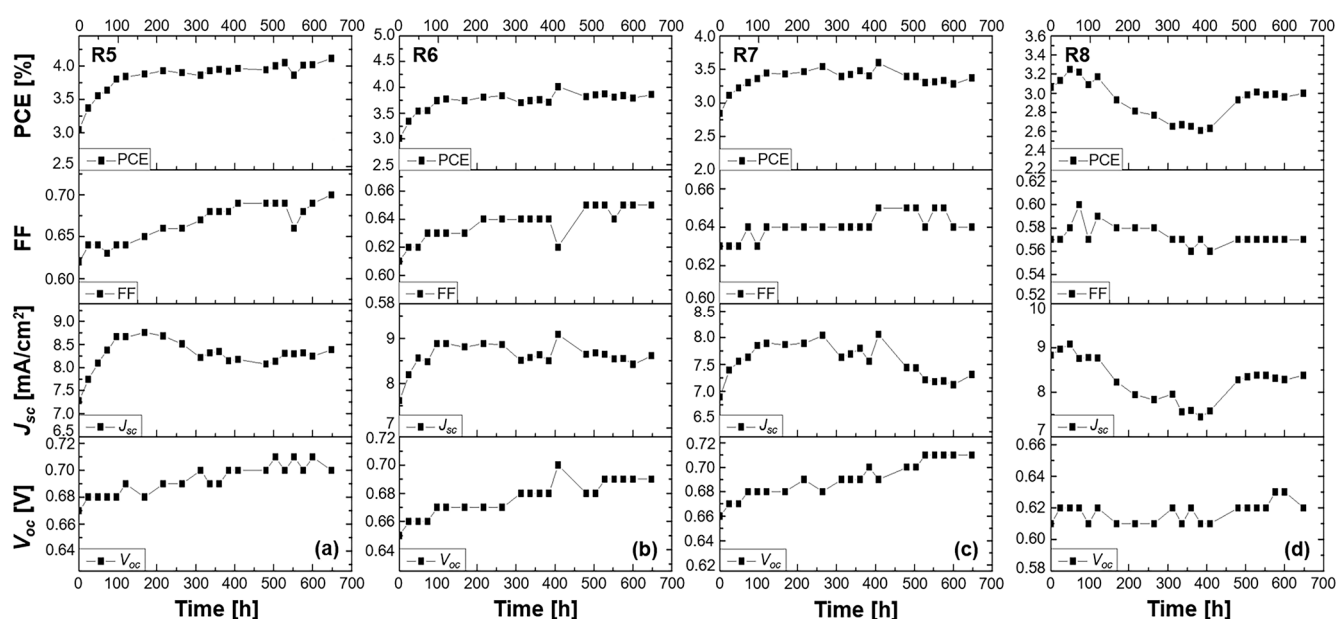


**Figure 5.** Stability study of 2-LBH-44 DSSCs measured under ambient conditions for over 600 h. Performance of (a) a liquid DMPII electrolyte-based DSSC (R5) and of QsDSSCs employing PVDF-HFP-based gel electrolytes with varying molecular weights: (b) R6—DMPII + PVH70, (c) R7—DMPII + PVH80, and (d) R8—DMPII + PVDF-HFP.

The reference cell (R5) with liquid DPMII electrolyte exhibited a significant increase in all performance parameters— $V_{oc}$ ,  $J_{sc}$ , FF, and PCE—after 650 h. This improvement could be attributed to factors like improved electrolyte infiltration into the mesoporous TiO<sub>2</sub> layer and enhanced interfacial contact between the dye and electrolyte, leading to better charge injection and collection. However, the long-term stability of liquid electrolytes remains a concern due to potential evaporation or leakage issues [25]. Incorporating PVDF-HFP significantly influenced the device's behavior. R6, with a lower-molecular-weight PVDF-HFP (86,000 g/mol), showed comparable performance enhancement to R5, suggesting that at this molecular weight, the polymer effectively enhanced ionic conductivity and interfacial contact, leading to increased  $V_{oc}$ ,  $J_{sc}$ , and FF, and consequently, PCE. R7, with a slightly higher molecular weight (90,000 g/mol), showed a decrease in  $J_{sc}$ , likely due to the polymer's increased viscosity hindering ionic transport. However, the  $V_{oc}$  and FF improvements, attributed to reduced recombination and enhanced electron lifetime, resulted in a moderate PCE increase. Interestingly, R8, with the highest molecular weight (455,000 g/mol), exhibited an initial increase in  $J_{sc}$ , possibly due to improved stability and reduced recombination; however, the  $J_{sc}$  experienced a subsequent decline, suggesting a trade-off between stability and charge transport limitations. The almost constant PCE in R8 indicates that while the high-molecular-weight polymer enhanced stability, it compromised charge transport, highlighting the need to optimize the polymer molecular weight for an optimal balance between these factors [26].

The use of 2-LBH-44 phenothiazine dye in combination with different-molecular-weight PVDF-HFP polymer electrolytes revealed to significantly enhance the stability and performance of QsDSSCs. However, the molecular weight of the polymer played a crucial role in determining the optimal balance between ionic conductivity, charge recombination, and mechanical stability. Medium-molecular-weight polymers (e.g., 86,000 g/mol) seemed to offer the best trade-off, resulting in the highest improvements in  $V_{oc}$ ,  $J_{sc}$ , FF, and PCE. Additional research should focus on refining the polymer matrix properties to further enhance ionic diffusion while maintaining low recombination rates for long-term device stability [27,28].

### 3.5. DSSCs with 2-Ryu-4 Phenothiazine Dye and with and Without PVDF-HFP with Different Molecular Weights in DPMII Electrolyte

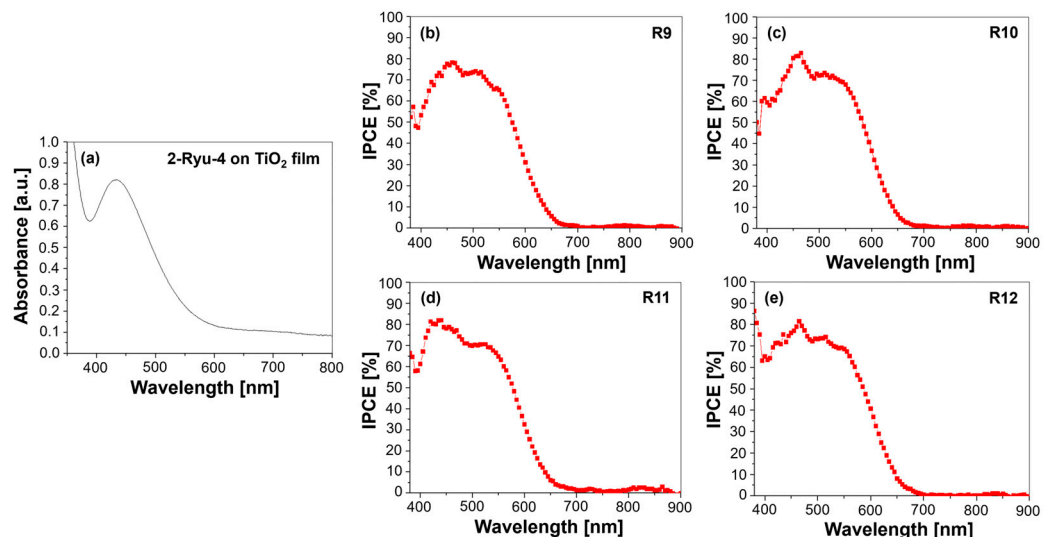
#### 3.5.1. UV-Vis Absorption and IPCE Spectra

Figure 6 presents the UV-Vis absorption spectrum of the (E)-2-cyano-3-(7-(4-(diphenylamino)phenyl)-10-hexyl-10H-phenothiazin-3-yl)acrylic acid (2-Ryu-4) dye adsorbed on a TiO<sub>2</sub> film and the IPCE spectra of various cells (R9-R12) with different electrolyte configurations.

The UV-Vis spectrum shows a broad absorption range from 400 to 700 nm (Figure 6a), peaking at approximately 470–500 nm, which correlates with strong  $\pi$ - $\pi^*$  transitions attributed to the phenothiazine core and diphenylamine unit. This broad absorption indicates effective light harvesting across a significant portion of the visible spectrum, essential for high-efficiency electron injection into the TiO<sub>2</sub> conduction band.

In contrast, the IPCE spectra (Figure 6b–e) provide insights into the quantum efficiency of photon conversion to electrical current across the same wavelength range. The onset of the IPCE curve typically aligns with the absorption onset observed in the UV-Vis spectrum; however, it is crucial to note that while the UV-Vis spectrum reflects light absorption capabilities, the IPCE spectrum indicates how effectively those absorbed photons are converted into electrical current. For instance, R9, using a DPMII-based liquid electrolyte without polymer, exhibited a peak IPCE of approximately 85% at around 500 nm, which closely matches the UV-Vis absorption peak. This alignment suggests efficient photon capture and electron injection. The introduction of PVDF-HFP polymer electrolytes modified these characteristics. Cells with PVH70 (R10) and PVH80 (R11) showed increased IPCE values peaking at 87 and 87.5%, respectively, indicating enhanced charge transport and reduced recombination losses due to improved electrolyte stability [26]. Notably, while these polymer-based cells maintained strong absorption in the visible region, their IPCE

profiles revealed a slight decline beyond 600 nm, reflecting limitations in light absorption in the NIR region. This discrepancy emphasizes that although a dye may have substantial absorption capabilities as indicated by UV–Vis spectra, its efficiency in converting absorbed photons into current may be affected by factors such as charge recombination dynamics and ionic conductivity within the electrolyte matrix.



**Figure 6.** (a) UV–Vis absorption spectrum of the 2-Ryu-4 phenothiazine dye adsorbed on a TiO<sub>2</sub> film and IPCE spectra for DSSCs employing 2-Ryu-4 with various electrolytes: (b) R9—DMPII, (c) R10—DMPII + PVH70, (d) R11—DMPII + PVH80, and (e) R12—DMPII + PVDF-HFP.

In summary, while both UV–Vis and IPCE spectra are critical for understanding DSSC performance, they serve different purposes: UV–Vis provides information on light absorption properties of the dye, while IPCE reveals how effectively that absorbed light is converted into electrical energy. The interplay between these two analyses underscores the importance of optimizing both dye structures and electrolyte compositions to enhance overall device efficiency.

### 3.5.2. Stability Study

The stability study under continuous illumination for more than 600 h of the DSSCs based on the 2-Ryu-4 phenothiazine dye and on the liquid DMPII electrolyte without and with the incorporation of varying-molecular-weight PVDF-HFP polymers revealed a complex interplay of factors influencing device performance (Figure 7).

The reference cell (R9) with liquid DPMII electrolyte showed an initial efficiency increase, likely due to improved electrolyte penetration and dye regeneration. However, the subsequent decrease in  $J_{sc}$  and overall efficiency suggested limitations in long-term stability, possibly due to electrolyte evaporation or degradation. The increase in FF could be attributed to improved charge collection, while the decrease in  $V_{oc}$  might indicate increased recombination or changes in the TiO<sub>2</sub>/dye/electrolyte interface. Incorporating PVDF-HFP led to distinct behavior depending on the molecular weight. Cells R10 and R11, with lower-molecular-weight PVDF-HFP (86,000 and 90,000 g/mol), exhibited an initial increase in  $V_{oc}$ , potentially due to passivation of TiO<sub>2</sub> surface traps, reducing recombination. However, the continuous decrease in  $J_{sc}$ , more pronounced with increasing molecular weight, suggested hindered charge transport due to increased electrolyte viscosity. This trade-off between reduced recombination (higher  $V_{oc}$  and FF) and hindered transport (lower  $J_{sc}$ ) resulted in an overall efficiency decrease. R12, with the highest molecular weight (455,000 g/mol), showed a consistent increase in  $V_{oc}$  and FF, indicating effective recombination suppression. However, the significant  $J_{sc}$  drop, likely due to severely hindered ionic transport, outweighed the positive impact on  $V_{oc}$  and FF, leading to an overall efficiency decrease. This highlights the critical challenge in QsDSSCs, i.e., balancing efficient charge transport

with long-term stability, thus emphasizing the need to optimize the polymer molecular weight and electrolyte composition for optimal device performance [29–31].

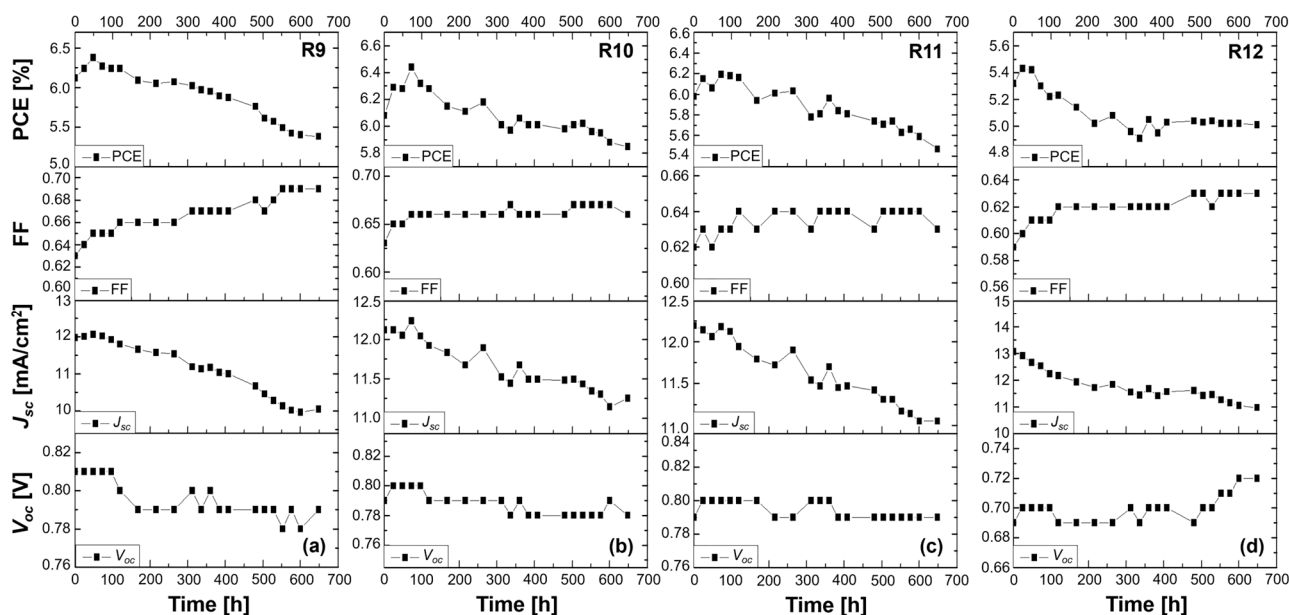


**Figure 7.** Stability study of 2-Ryu-4 DSSCs measured under ambient conditions for over 600 h. Performance of (a) a liquid DMPII electrolyte-based DSSC (R9) and of QsDSSCs employing PVDF-HFP-based gel electrolytes with different molecular weights: (b) R10—DMPII + PVH70, (c) R11—DMPII + PVH80, and (d) R12—DMPII + PVDF-HFP.

Among the four solar cells sensitized with the 2-Ryu-4 phenothiazine dye, the R12 cell, incorporating the highest-molecular-weight PVDF-HFP polymer in the DMPII liquid electrolyte, showed the most promising long-term stability (Figure 7d) [8,30,32,33]. The higher-molecular-weight polymer provided a more rigid and stable matrix, which effectively suppressed the leakage of the liquid electrolyte components and enhanced the mechanical integrity of the device [30]. Moreover, it led to more efficient electron transport and reduced charge recombination at the  $\text{TiO}_2$ /electrolyte interface [30]. Additionally, the increased viscosity of the electrolyte reduced the diffusion rate of the redox species and the light harvesting efficiency of the dye, leading to a decrease in the  $J_{sc}$ .

In summary, the findings of the stability study depicted in Figure 7 highlight, at the same time, the potential of 2-Ryu-4 phenothiazine dye and polymer electrolytes for the development of stable and efficient QsDSSCs and the crucial role of the polymer electrolyte composition and molecular weight in determining their performance and long-term stability. The use of a high-molecular-weight PVDF-HFP polymer not only improved the mechanical integrity and sealing of the device but also enhanced the charge transport and reduced recombination, leading to a significant improvement in the overall long-term stability. The reduction in PCE for all the cells R9–R12, instead, was ascribed to the increased viscosity of the polymer electrolyte, which reduced the effective diffusion of the redox species and the charge transport, as described in previous studies [30,34,35].

#### 4. Discussion

The performance of QsDSSCs utilizing phenothiazine-based organic dyes—specifically, 2-LBH-100, 2-LBH-44, and 2-Ryu-4—has been rigorously analyzed through  $J$ – $V$  characteristics, stability studies, and quantum efficiency assessments. Each dye exhibited unique performance profiles influenced by molecular structure, electrolyte choice, and polymer incorporation.

For 2-LBH-100, the  $J$ – $V$  characteristics revealed an increase in  $V_{oc}$  and FF when using the liquid DMPII electrolyte, with  $V_{oc}$  rising by 3% and FF enhancing due to improved

charge collection efficiency. However, the significant decrease in  $J_{sc}$  over time highlighted a trade-off between initial performance gains and long-term stability challenges. In contrast, 2-LBH-44 demonstrated a broader absorption spectrum with notable IPCE, effectively harvesting light across 400–700 nm. The presence of a lower-molecular-weight PVDF-HFP polymer (e.g., PVH70) positively influenced  $V_{oc}$  but resulted in decreased  $J_{sc}$  due to increased viscosity and potential dye aggregation within the polymer matrix. For 2-Ryu-4, the stability study indicated a complex relationship between  $V_{oc}$  and  $J_{sc}$ . While  $V_{oc}$  initially showed slight improvements,  $J_{sc}$  significantly decreased after prolonged exposure to ambient conditions. This behavior emphasizes the necessity of optimizing polymer characteristics to mitigate degradation effects while enhancing charge transport dynamics.

Long-term stability studies for over 600 h revealed critical insights into environmental resilience. For instance, the R9 cell with liquid DMPII electrolyte exhibited a 3.7% decrease in  $V_{oc}$  but an 8.4% increase in FF, suggesting improved charge collection despite some voltage degradation. However, the substantial 21% decrease in  $J_{sc}$  pointed to potential issues with dye stability or ionic mobility within the electrolyte. In formulations with PVDF-HFP, such as R10 (molecular weight 86,000 g/mol), an initial increase in  $V_{oc}$  by 1.5% was followed by a decline of 3%. Although FF improved by 4%, this indicated that while lower-molecular-weight polymers enhanced interfacial contact, they may not sufficiently protect against dye degradation over time. Similarly, R11 (90,000 g/mol) showed stabilized  $V_{oc}$  after an initial increase but experienced a consistent decline in  $J_{sc}$  by 9.6%, resulting in an overall efficiency drop of 8%. These results suggest that while polymer interactions can enhance performance metrics initially, they may lead to long-term challenges if they do not adequately protect the dye from environmental factors. The highest-molecular-weight formulation (R12 with PVDF-HFP at 455,000 g/mol) displayed an intriguing pattern:  $V_{oc}$  increased by 5% and FF improved by 6%, yet  $J_{sc}$  decreased by 15%, leading to an overall efficiency decrease of 6%. This suggests that higher-molecular-weight polymers may create a rigid structure that inhibits ionic mobility and reduces effective charge transport pathways despite voltage and fill factor improvements.

The quantum efficiency spectra further elucidated each dye's ability to convert absorbed photons into electrical current. Notably, QsDSSCs containing 2-LBH-44 demonstrated high peak efficiencies closely correlating with their UV-Vis absorption spectra, indicating efficient charge separation and transport mechanisms. Lower-molecular-weight PVDF-HFP formulations enhanced IPCE across a broader spectral range compared to their higher-molecular-weight counterparts.

In summary, the analysis of QsDSSCs utilizing phenothiazine-based dyes underscored the intricate interplay between dye chemistry, electrolyte composition, and polymer characteristics in determining device efficiency and stability. Enhancements in  $V_{oc}$  and FF must be balanced with  $J_{sc}$  to ensure comprehensive improvements in solar cell performance. Future work should focus on optimizing polymer formulations for mechanical stability and ionic conductivity while protecting the dye from degradation. Exploring alternative materials or additives could further enhance both stability and efficiency, contributing valuable insights for future innovations in renewable energy technologies.

## 5. Conclusions

This study investigated the intricate relationship between dye chemistry, electrolyte composition, and polymer properties in QsDSSCs. Focusing on phenothiazine-based organic dyes (2-LBH-100, 2-LBH-44, and 2-Ryu-4), this research revealed the key factors influencing device performance and stability. While these dyes demonstrated promising light-harvesting capabilities, their photovoltaic performance was significantly affected by the electrolyte choice and the molecular weight of the PVDF-HFP polymer additive. Variations in open-circuit voltage, short-circuit current density, fill factor, and power conversion efficiency underscored the need for parameter optimization. 2-LBH-100, for example, showed improved  $V_{oc}$  and FF with a liquid DMPII electrolyte, suggesting enhanced charge separation. However, long-term stability tests revealed declining  $J_{sc}$  and efficiency after



more than 600 h, indicating potential dye degradation or electrolyte instability. Further investigation into these degradation mechanisms is warranted, potentially using techniques like impedance or transient absorption spectroscopy. 2-LBH-44's performance, initially promising due to its broad absorption and high incident photon-to-current conversion efficiency, was negatively impacted by the increased viscosity of higher-molecular-weight PVDF-HFP, hindering ionic mobility and reducing  $J_{sc}$ . This highlights the importance of balancing polymer properties for optimal electrolyte performance. Alternative polymer additives or optimized polymer concentrations could improve device performance. The complex  $V_{oc}$ - $J_{sc}$  relationship observed for 2-Ryu-4 further emphasizes the need for careful polymer optimization. While some formulations improved  $V_{oc}$ , the significant  $J_{sc}$  drops suggested a performance trade-off. Analyzing charge transport and recombination dynamics could provide further insights. This work advances QsDSSC technology by elucidating critical factors influencing performance and stability. Future research should focus on novel polymer blends with improved ionic conductivity and dye compatibility, strategies to enhance dye stability, and alternative device architectures, such as incorporating hole transport layers or different photoanode materials. Addressing these challenges will significantly advance the commercial viability of QsDSSCs.

**Author Contributions:** Conceptualization, R.A.A., K.Y.R., W.S.S. and D.P.; methodology, R.A.A., K.Y.R., W.S.S. and D.P.; formal analysis, R.A.A., K.Y.R., W.S.S. and D.P.; data curation, R.A.A., K.Y.R. and W.S.S.; writing—original draft preparation, R.A.A., W.S.S. and D.P.; writing—review and editing, R.A.A., W.S.S. and D.P.; visualization, R.A.A., W.S.S. and D.P.; supervision, W.S.S.; project administration, R.A.A. and W.S.S.; funding acquisition, R.A.A. and W.S.S. All authors have read and agreed to the published version of the manuscript.

**Funding:** This study was supported by the Converging Research Center Program through the Ministry of Education, Science, and Technology (2010K000970), Republic of Korea.

**Data Availability Statement:** Data are available on request due to privacy restrictions.

**Acknowledgments:** R.A.A. would like to thank Sunandan Baruah for the fruitful discussions. D.P. acknowledges the support from the European Union—NextGenerationEU under the National Recovery and Resilience Plan (NRRP), Mission 04 Component 2 Investment 3.1 | Project Code: IR0000027—CUP: B33C22000710006—iENTRANCE@ENL: Infrastructure for Energy TRAnsition aNd Circular Economy @EuroNanoLab.

**Conflicts of Interest:** The authors declare no conflicts of interest.

## References

1. O'Regan, B.; Grätzel, M. A low-cost, high-efficiency solar cell based on dye-sensitized colloidal  $\text{TiO}_2$  films. *Nature* **1991**, *353*, 737–740. [[CrossRef](#)]
2. Saidi, N.M.; Omar, F.S.; Numan, A.; Apperley, D.C.; Algaradah, M.M.; Kasi, R.; Avestro, A.-J.; Subramaniam, R.T. Enhancing the efficiency of a dye-sensitized solar cell based on a metal oxide nanocomposite gel polymer electrolyte. *ACS Appl. Mater. Interfaces* **2019**, *11*, 30185–30196. [[CrossRef](#)]
3. Pang, H.-W.; Yu, H.-F.; Huang, Y.-J.; Li, C.-T.; Ho, K.-C. Electrospun membranes of imidazole-grafted PVDF-HFP polymeric ionic liquids for highly efficient quasi-solid-state dye-sensitized solar cells. *J. Mater. Chem. A* **2018**, *6*, 14215–14223. [[CrossRef](#)]
4. Li, C.; Xin, C.; Xu, L.; Zhong, Y.; Wu, W. Components control for high-voltage quasi-solid state dye-sensitized solar cells based on two-phase polymer gel electrolyte. *Sol. Energy* **2019**, *181*, 130–136. [[CrossRef](#)]
5. Day, J.; Senthilarasu, S.; Mallick, T.K. Improving spectral modification for applications in solar cells: A review. *Renew. Energy* **2019**, *132*, 186–205. [[CrossRef](#)]
6. Agarwal, R.; Vyas, Y.; Chundawat, P.; Dharmendra; Ameta, C. Outdoor performance and stability assessment of dye-sensitized solar cells (DSSCs). In *Solar Radiation—Measurement, Modeling and Forecasting Techniques for Photovoltaic Solar Energy Applications*; Aghaei, M., Ed.; IntechOpen: London, UK, 2022; pp. 1–21.
7. Zhang, D.; Stojanovic, M.; Ren, Y.; Cao, Y.; Eickemeyer, F.T.; Socie, E.; Vlachopoulos, N.; Moser, J.-E.; Zakeeruddin, S.M.; Hagfeldt, A.; et al. A molecular photosensitizer achieves a  $V_{oc}$  of 1.24 V enabling highly efficient and stable dye-sensitized solar cells with copper(II/I)-based electrolyte. *Nat. Commun.* **2021**, *12*, 1777. [[CrossRef](#)] [[PubMed](#)]
8. Sharma, K.; Sharma, V.; Sharma, S.S. Dye-sensitized solar cells: Fundamentals and current status. *Nanoscale Res. Lett.* **2018**, *13*, 381. [[CrossRef](#)]

9. Al-Busaidi, I.J.; Haque, A.; Al Rasbi, N.K.; Khan, M.S. Phenothiazine-based derivatives for optoelectronic applications: A review. *Synth. Met.* **2019**, *257*, 116189. [[CrossRef](#)]
10. Almenningen, D.M.; Haga, B.S.; Hansen, H.E.; Buene, A.F.; Hoff, B.H.; Gautun, O.R. Adamantyl side chains as anti-aggregating moieties in dyes for dye-sensitized solar cells. *Chem. Eur. J.* **2022**, *28*, e202201726. [[CrossRef](#)]
11. Li, S.; He, J.; Jiang, H.; Mei, S.; Hu, Z.; Kong, X.; Yang, M.; Wu, Y.; Zhang, S.; Tan, H. Comparative studies on the structure–performance relationships of phenothiazine-based organic dyes for dye-sensitized solar cells. *ACS Omega* **2021**, *6*, 6817–6823. [[CrossRef](#)]
12. Santos, H.F.; Dos Santos, C.G.; Nascimento, O.R.; Reis, A.K.C.A.; Lanfredi, A.J.C.; De Oliveira, H.P.M.; Nantes-Cardoso, I.L. Charge separation of photosensitized phenothiazines for applications in catalysis and nanotechnology. *Dyes Pigm.* **2020**, *177*, 108314. [[CrossRef](#)]
13. Gong, P.; An, L.; Tong, J.; Liu, X.; Liang, Z.; Li, J. Design of A-D-A-type organic third-order nonlinear optical materials based on benzodithiophene: A DFT study. *Nanomaterials* **2022**, *12*, 3700. [[CrossRef](#)]
14. Choi, H.; Paek, S.; Lim, K.; Kim, C.; Kang, M.-S.; Song, K.; Ko, J. Molecular engineering of organic sensitizers for highly efficient gel-state dye-sensitized solar cells. *J. Mater. Chem. A* **2013**, *1*, 8226–8233. [[CrossRef](#)]
15. Afre, R.A.; Ryu, K.Y.; Shin, W.S.; Pugliese, D. Comparative study of quasi-solid-state dye-sensitized solar cells using Z907, N719, photoactive phenothiazine dyes and PVDF-HFP gel polymer electrolytes with different molecular weights. *Photonics* **2024**, *11*, 760. [[CrossRef](#)]
16. Yang, X.; Zhao, J.; Wang, L.; Tian, J.; Sun, L. Phenothiazine derivatives-based D- $\pi$ -A and D-A- $\pi$ -A organic dyes for dye-sensitized solar cells. *RSC Adv.* **2014**, *4*, 24377–24383. [[CrossRef](#)]
17. Wu, Y.; Zhu, W. Organic sensitizers from D- $\pi$ -A to D-A- $\pi$ -A: Effect of the internal electron-withdrawing units on molecular absorption, energy levels and photovoltaic performances. *Chem. Soc. Rev.* **2013**, *42*, 2039–2058. [[CrossRef](#)] [[PubMed](#)]
18. Mishra, A.; Fischer, M.K.R.; Bäuerle, P. Metal-free organic dyes for dye-sensitized solar cells: From structure: Property relationships to design rules. *Angew. Chem. Int. Ed.* **2009**, *48*, 2474–2499. [[CrossRef](#)]
19. Ye, M.; Wen, X.; Wang, M.; Iocozzia, J.; Zhang, N.; Lin, C.; Lin, Z. Recent advances in dye-sensitized solar cells: From photoanodes, sensitizers, and electrolytes to counter electrodes. *Mater. Today* **2015**, *18*, 155–162. [[CrossRef](#)]
20. Lee, K.-M.; Suryanarayanan, V.; Ho, K.-C. A photo-physical and electrochemical impedance spectroscopy study on the quasi-solid state dye-sensitized solar cells based on poly(vinylidene fluoride-co-hexafluoropropylene). *J. Power Sources* **2008**, *185*, 1605–1612. [[CrossRef](#)]
21. Duvva, N.; Eom, Y.K.; Reddy, G.; Schanze, K.S.; Giribabu, L. Bulky phenanthroimidazole–phenothiazine D- $\pi$ -A based organic sensitizers for application in efficient dye-sensitized solar cells. *ACS Appl. Energy Mater.* **2020**, *3*, 6758–6767. [[CrossRef](#)]
22. Masud; Kim, K.M.; Kim, H.K. Polymer gel electrolytes based on PEG-functionalized ABA triblock copolymers for quasi-solid-state dye-sensitized solar cells: Molecular engineering and key factors. *ACS Appl. Mater. Interfaces* **2020**, *12*, 42067–42080. [[CrossRef](#)]
23. Han, F.; Wang, Y.; Wan, Z.; Jia, C.; Luo, J.; Yao, X. Enhanced photovoltaic performances of dye-sensitized solar cells sensitized with D-D- $\pi$ -A phenothiazine-based dyes. *Synth. Met.* **2016**, *221*, 95–102. [[CrossRef](#)]
24. Sharma, G.D.; Suresh, P.; Roy, M.S.; Mikroyannidis, J.A. Effect of surface modification of TiO<sub>2</sub> on the photovoltaic performance of the quasi solid state dye sensitized solar cells using a benzothiadiazole-based dye. *J. Power Sources* **2010**, *195*, 3011–3016. [[CrossRef](#)]
25. Shen, S.-Y.; Dong, R.-X.; Shih, P.-T.; Ramamurthy, V.; Lin, J.-J.; Ho, K.-C. Novel polymer gel electrolyte with organic solvents for quasi-solid-state dye-sensitized solar cells. *ACS Appl. Mater. Interfaces* **2014**, *6*, 18489–18496. [[CrossRef](#)] [[PubMed](#)]
26. Bandara, T.M.W.J.; Weerasinghe, A.M.J.S.; Dissanayake, M.A.K.L.; Senadeera, G.K.R.; Furlani, M.; Albinsson, I.; Mellander, B.-E. Characterization of poly (vinylidene fluoride-co-hexafluoropropylene) (PVdF-HFP) nanofiber membrane based quasi solid electrolytes and their application in a dye sensitized solar cell. *Electrochim. Acta* **2018**, *266*, 276–283. [[CrossRef](#)]
27. Cao, Y.; Saygili, Y.; Ummadisingu, A.; Teuscher, J.; Luo, J.; Pellet, N.; Giordano, F.; Zakeeruddin, S.M.; Moser, J.-E.; Freitag, M.; et al. 11% efficiency solid-state dye-sensitized solar cells with copper (II/I) hole transport materials. *Nat. Commun.* **2017**, *8*, 15390. [[CrossRef](#)]
28. Cheng, Y.; Yang, G.; Jiang, H.; Zhao, S.; Liu, Q.; Xie, Y. Organic sensitizers with extended conjugation frameworks as cosensitizers of porphyrins for developing efficient dye-sensitized solar cells. *ACS Appl. Mater. Interfaces* **2018**, *10*, 38880–38891. [[CrossRef](#)] [[PubMed](#)]
29. Ito, S. Investigation of dyes for dye-sensitized solar cells: Ruthenium-complex dyes, metal-free dyes, metal-complex porphyrin dyes and natural dyes. In *Solar Cells—Dye-Sensitized Devices*, 1st ed.; Kosyachenko, L.A., Ed.; IntechOpen: London, UK, 2011; pp. 19–48.
30. Law, C.H.; Pathirana, S.C.; Li, X.; Anderson, A.Y.; Barnes, P.R.F.; Listorti, A.; Ghaddar, T.H.; O'Regan, B.C. Water-based electrolytes for dye-sensitized solar cells. *Adv. Mater.* **2010**, *22*, 4505–4509. [[CrossRef](#)]
31. Roy, M.S.; Deol, Y.S.; Kumar, M.; Prasad, N.; Janu, Y. Dye-sensitized solar cells for solar energy harvesting. *AIP Conf. Proc.* **2011**, *1391*, 46–49.
32. Gong, J.; Sumathy, K.; Qiao, Q.; Zhou, Z. Review on dye-sensitized solar cells (DSSCs): Advanced techniques and research trends. *Renew. Sustain. Energy Rev.* **2017**, *68*, 234–246. [[CrossRef](#)]
33. Li, J.; Shi, Y. Electron Transport and Recombination in TiO<sub>2</sub> Nanofiber Dye Sensitized Solar Cell. In Proceedings of the ASME 2011 International Mechanical Engineering Congress and Exposition, Denver, CO, USA, 11–17 November 2011.

34. Cha, S.Y.; Lee, Y.-G.; Kang, M.-S.; Kang, Y.S. Correlation between ionic conductivity and cell performance in solid-state dye-sensitized solar cells employing polymer electrolyte. *J. Photochem. Photobiol.* **2010**, *211*, 193–196. [[CrossRef](#)]
35. Kim, J.Y.; Kim, T.H.; Kim, D.Y.; Park, N.-G.; Ahn, K.-D. Novel thixotropic gel electrolytes based on dicationic bis-imidazolium salts for quasi-solid-state dye-sensitized solar cells. *J. Power Sources* **2008**, *175*, 692–697. [[CrossRef](#)]

**Disclaimer/Publisher’s Note:** The statements, opinions and data contained in all publications are solely those of the individual author(s) and contributor(s) and not of MDPI and/or the editor(s). MDPI and/or the editor(s) disclaim responsibility for any injury to people or property resulting from any ideas, methods, instructions or products referred to in the content.